Braz J Phys (2012) 42:391–399
DOI 10.1007/s13538-012-0102-1

SBF SOCIEDADE BRASILEIRA DE FÍSICA

NUCLEAR PHYSICS

Cluster Model Analysis of Kaon Scattering from ^{12}C

Ahmed A. Ebrahim

Received: 25 January 2012 / Published online: 8 November 2012

Abstract Angular distributions of differential cross sections for the interaction of K^+ mesons with ^{12}C nucleus at beam momenta of 635, 715, and 800 MeV/c have been analyzed using 3α-particle model of ^{12}C. Differential cross sections for inelastic transitions to the 2^+ (4.44 MeV) and 3^- (9.64 MeV) states in ^{12}C are calculated, and deformation lengths δ_2 and δ_3 are extracted and consistent with other works. Good agreement with experimental data of elastic and inelastic $K^{\pm}$-^{12}C scattering is obtained.

Keywords Kaon-nucleus scattering · Cluster model · Distorted wave theory · Nuclear models

1 Introduction

The K^+-nucleus scattering is of considerable interest due to the relatively weak kaon nucleon (KN) interaction. K^+-nucleus cross sections should be fairly weak and the amplitudes reasonably simple because of the simplicity of K^+N system. The K^+-nucleus interaction is the weakest of any strongly interacting probe, and the resulting mean free path is expected to be large (of the order of 7 *fm*). Therefore, K^+ can penetrate quite freely into the central region of the target nucleus, having time to undergo predominantly single K^+N collisions and appearing to be a good probe for the distribution of neutrons in nuclei, while electron scattering is applied to study the nuclear charge density. There is no true absorption of K^+ to complicate things, in distinction to the case of low energy π-nucleus scattering, where the mean free path is also large. Another difference is that K^+ wavelengths are small enough to sense individual nucleons within nuclei, where $\lambda = 2$ *fm* for 50 MeV pion kinetic energy while $\lambda = 0.5$ *fm* for 715 MeV/c kaon lab momentum [1].

On the contrary, the K^-N system has many narrow resonances ($\Gamma \simeq$ 15–40 MeV) and there are open channels down to the K^-N threshold. Cross sections are comparable to those for NN scattering. Therefore, we expect the K^--nucleus cross sections to reflect these features: The interaction is strong and the amplitudes are expected to be complicated [2].

An earlier elastic scattering experiment at 800 MeV/c [2] has gained interest since its results are higher than expected by optical potential model calculations. This led to the concept of "swollen nucleons," with the elementary projectile-nucleon coupling within the nucleus greater than that found in free space. Agreement in magnitude is found for an enhancement of the fundamental cross section by 33 % [3]. Since, however, the normalization uncertainty of that elastic scattering experiment was about 19 %, some of this theoretical enhancement may not be necessary. Total cross sections for K^+ mesons on several nuclei at a range of kaon lab momenta also exceeded model expectations [4, 5], indicating that nucleons within nuclear medium do not behave as they do in free space. These were analyzed by Siegel et al. [5] with the conclusion that agreement with theory is possible. In addition, there may be errors in the KN phase shifts used, although the agreement with the K^+-^{40}Ca results indicate these are not major. By comparing K^+-^{12}C results with K^+-deuterium scattering, the effects of

A. A. Ebrahim (✉)
Physics Department, Assiut University, Assiut 71516, Egypt
e-mail: aebrahim@aun.edu.eg

such errors are reduced. Siegel et al. [5] suggest that within the nucleus, there is an increase of the S11 KN phase shift relative to that given by Martin [2]. Two explanations have been offered. Siegel et al. suggest that the effect arises from an increase of nucleon size. Brown et al. [6] ascribe this increase to change in the mass of the ρ and ω which mediate the K^+ reaction in the nuclear medium. This leads to an optical potential that depends nonlinearly on the nucleon density giving rise to an increased repulsion (over the first-order $t\rho$) and a decreased effective nuclear radius. The agreement with experiment can be obtained by changing the mass of ρ and ω in the nuclear medium.

The kaon-nucleus optical potential is based on the K^+N t-matrix and the nuclear one-particle wave functions of a square well potential [7]. The agreement with experimental data was obtained with increasing the S11 K^+N phase shift by 10–15 % which is taken as in-medium effect. Also, K^+ has been studied scattering with a local version [8] of the Kisslinger potential [9]. This has been early suggested for pion-nucleus scattering. A 6-parameter Woods–Saxon potential is fitted to experimental data [10]. However, ambiguities appear in the values of these parameters when adjusted to experimental data. When inelastic calculations are forced to give the known transition strengths, the ambiguity in parameters can be removed.

Recently, coupled-channels calculations for elastic and inelastic scattering of K^+ at 715 MeV/c by ^{6}Li and ^{12}C at 635, 715, and 800 MeV/c kaon lab momenta have been analyzed [11], using the Watanabe superposition model in a Woods–Saxon shape, together with coupled-channels Born approximation. This was carried out in terms of alpha-particle and deuteron optical potentials, taking into account alpha-deuteron and 3α-clusters of ^{6}Li and ^{12}C nuclei. The elastic scattering studies resulted in considerable ambiguities in Woods–Saxon (WS) parameters. Using best fit parameters, calculations were carried out for inelastic scattering of kaons to the lowest 2^+ and 3^- states of ^{12}C and 3^+ of ^{6}Li. The corresponding deformation parameters were extracted, and ambiguities in WS parameters were greatly reduced. It was concluded that the Watanabe superposition model in WS potential form seems to be useful for kaon-nucleus scattering.

In the present work, the distorted wave Born approximation (DWBA) is applied for the interaction between the projectile and the whole target nucleus. We derive an optical potential for the reaction $K^{\pm}$-^{12}C when the nucleus is considered to be constructed of three alpha clusters together with the DWUCK4 code [12]. The derived optical potential is employed to successfully predict the angular distributions of the differential cross sections of the $K^{\pm}$ elastically and inelastically scattered to the lowest 2^+ and 3^- states in ^{12}C in the momentum range of 635–800 MeV/c.

2 The Folding Model

The DWUCK4 code which solves the nonrelativistic Schrödinger equation, and was originally written to calculate the scattering and reaction observables for binary nuclear reactions, is used to calculate the angular distribution for kaon scattering from a nucleus. Such a program should be provided with an effective kaon mass, the target mass and an effective kaon energy. This requires transforming the true kaon mass m_K and beam energy T_K to surrogate values E_L and M_K [13], using $M_K = \gamma_K m_K$ with m_K the free charged kaon mass of 0.530 amu or 493.707 MeV and

$$\gamma_K = (x + \gamma_L)/(1 + x^2 + 2x\gamma_L)^{1/2}, \qquad x = m_K/m_T,$$
$$\gamma_L = 1 + (T_K/m_K c^2).$$

Here, m_T = target mass = A times the amu. It is convenient to use the center of mass kinetic energy $E_{cm} = 20.901\, k^2\, (M_K + m_T)/M_K m_T$ MeV, with M_K and m_T in amu, with $k = (m_K c/\hbar)\sqrt{(\gamma_K^2 - 1)}$, giving $E_L = E_{cm}\,(M_K + m_T)/m_T$.

As an example, for a $T_K = 310.638$ MeV ($P_{\text{lab}} = 635$ MeV/c) charged kaon incident upon ^{12}C, one replaces the true kaon mass into the DWUCK4 code with $M_K = 0.82852$ amu $= 771.6$ MeV, and the actual beam energy with $E_L = 260.54$ MeV. A parameter-free version of the local potential method has been applied with good success to a limited range of kaon-nucleus data [8].

^{12}C is considered to consist of three α-particles; each α-particle is bound much more weakly than a nucleon in the ^{12}C nucleus. In the following, we derive an analytical expression of $K^{\pm}$-^{12}C potential with the 3α-cluster model of ^{12}C. The resulting potential is inserted into the DWUCK4 code to calculate the differential cross sections. The calculations are compared to experimental data [2, 14].

The total optical potential of $K^{\pm} - \alpha$ scattering can be described in the usual WS radial dependence

$$V_\alpha(R) = V_C(R) - U_N(R), \tag{1}$$

where R is the separation distance between the kaon and α-particle, V_C(R) is the Coulomb potential which is taken to be that of a uniform charged sphere of radius

$R_C = 1.2\, A^{1/3}\, fm$ [15], and A is the target mass number. The nuclear potential $U_N(R)$ is defined to be

$$U_N(R) = V\, f(R, R_v, a_v) + i\, W\, f(R, R_w, a_w),$$

where $f(R, R_i, a_i) = [1 + \exp(R - R_i)/a_i]^{-1}$ $(i = v, w)$ is the Woods–Saxon function. V, $R_v (= r_v\, A^{1/3})$, and a_v are, respectively, the depth, radius, and diffuseness of the real part of the potential and W, $R_w (= r_w\, A^{1/3})$, and a_w are the corresponding quantities for the imaginary part. Since kaons are spinless particles, the spin-orbit term is not taken into account.

To fit the experimental distributions, the optical model parameters were varied systematically to minimize the quantity:

$$\chi^2 = \frac{1}{N} \sum_{i=1}^{N} \left(\frac{\sigma_{exp}(\theta_i) - \sigma_{th}(\theta_i)}{\Delta\sigma_{exp}(\theta_i)} \right)^2, \tag{2}$$

where N is the total number of the experimental points, $\sigma_{th}(\theta_i)$ is the predicted differential cross section at angle θ_i, and $\sigma_{exp}(\theta_i)$ and $\Delta\sigma_{exp}(\theta_i)$ are the experimental cross section and its associated error, respectively, where relative errors of 10 % [16–18] were taken for computing χ^2.

In the framework of folding model, we can take the interaction between $K^{\pm}$ and α-particle as the elementary interaction to fold the α-particle density of the target nucleus ^{12}C, and then obtain a single folding potential as

$$\begin{aligned} V_{^{12}C}(R) = \int |\, \psi(r, \rho)\, |^2 \\ \times \left[V_\alpha \left(\left| \bar{R} + \frac{2}{3}\bar{\rho} \right| \right) + V_\alpha \left(\left| \bar{R} - \frac{1}{3}\bar{\rho} - \frac{1}{2}\bar{r} \right| \right) \right. \\ \left. + V_\alpha \left(\left| \bar{R} - \frac{1}{3}\bar{\rho} + \frac{1}{2}\bar{r} \right| \right) \right] d\bar{r}\, d\bar{\rho}, \end{aligned} \tag{3}$$

where $\bar{R}$ is the separation vector between the centers of the two colliding particles. The internal position vectors $\bar{r}$ and $\bar{\rho}$ are defined by the position vectors of the three alpha particles $\bar{R}_1$, $\bar{R}_2$, and $\bar{R}_3$ constituting ^{12}C nucleus so that

$$\bar{r} = \bar{R}_2 - \bar{R}_1 \quad \text{and} \quad \bar{\rho} = \bar{R}_3 - \frac{1}{2}\left(\bar{R}_1 + \bar{R}_2\right).$$

The nuclear matter density distribution for α-particle

$$\rho_\alpha(r) = \rho_0\, \exp\left(-\beta\, r^2\right), \tag{4}$$

where $\rho_0 = 0.4229\, fm^-$ and $\beta = 0.0.7014\, fm^{-2}$ [19].

The optical potential of each kaon-alpha in ^{12}C is given by V_α. The internal wave function of ^{12}C has the form [20]

$$\psi(r, \rho) = \left(\frac{2\sqrt{3}\,\mu}{\pi} \right)^{\frac{3}{2}} \exp\left(-\mu \left(2\,\rho^2 + \frac{3}{2}\, r^2 \right) \right), \tag{5}$$

where μ is the range parameter of ^{12}C discussed below in Section 3. We can decompose (3) into:

$$V_{^{12}C}(R) = V_{\alpha 1}(R) + V_{\alpha 2}(R) + V_{\alpha 3}(R), \tag{6}$$

where

$$V_{\alpha 1}(R) = \int |\, \psi(r, \rho)\, |^2 \left[V_\alpha \left(\left| \bar{R} + \frac{2}{3}\,\bar{\rho} \right| \right) \right] d\bar{r}\, d\bar{\rho},$$

$$V_{\alpha 2}(R) = \int |\, \psi(r, \rho)\, |^2 \left[V_\alpha \left(\left| \bar{R} - \frac{1}{3}\,\bar{\rho} - \frac{1}{2}\,\bar{r} \right| \right) \right] d\bar{r}\, d\bar{\rho},$$

and

$$V_{\alpha 3}(R) = \int |\, \psi(r, \rho)\, |^2 \left[V_\alpha \left(\left| \bar{R} - \frac{1}{3}\,\bar{\rho} + \frac{1}{2}\,\bar{r} \right| \right) \right] d\bar{r}\, d\bar{\rho}. \tag{7}$$

Since $\psi(r, \rho)$ depends explicitly on the spatial coordinates r and ρ and $\psi(r, \rho)$ is spatially symmetric about the exchange of nucleons [21], the integral is not changed if the carbon coordinate system is reoriented each time so that the α cluster, which is being folded, lies along the vector $\bar{\rho}$. This allows the potential to be written as

$$\begin{aligned} V_{^{12}C}(R) &= 3\, V_{\alpha 1}(R). \\ &= 3 \int |\, \psi(r, \rho)\, |^2\, V_\alpha \left(\left| \bar{R} + \frac{2}{3}\,\bar{\rho} \right| \right) d\bar{r}\, d\bar{\rho}. \end{aligned} \tag{8}$$

Replacing the variable $\bar{\rho}$ by $\bar{y}$ defined by $(\bar{y} = \bar{R} + \frac{2}{3}\bar{\rho})$ and taking $\bar{R}$ as the polar axis for the angle integration with respect to $\bar{y}$

$$\begin{aligned} V_{^{12}C}(R) = \frac{8\sqrt{\mu}}{\sqrt{\pi}\, R} e^{-9\mu R^2} \\ \times \int_0^\infty dy y e^{-9\mu y^2}\, V_\alpha(y) \sinh(18\mu y R). \end{aligned} \tag{9}$$

The radial parts of the hadronic inelastic transition potential used here are:

$$F_l(R) = -\delta_l\, \frac{dV_{^{12}C}(R)}{dR}, \tag{10}$$

where $V_{^{12}C}$(R) is the optical potential found to fit the corresponding elastic scattering (9). For a given transition, we use δ_l to denote the corresponding real and imaginary "deformation lengths" for the $K^{\pm}$ interaction, while l(=2 or 3) is the multipolarity; δ_2 denotes the corresponding deformation length for the transition to

Table 1 The phenomenological optical potential parameters for α-particles, they are parameterized in a Woods–Saxon form

Reaction	P_{lab} (MeV/c)	V (MeV)	r_v (fm)	a_v (fm)	W (MeV)	r_w (fm)	a_w (fm)
$K^{\pm}$-α	635	56.58	1.075	0.538	45.32	0.923	0.483
	715	80.32	1.221	0.605	42.05	0.904	0.403
	800	100.25	1.025	0.502	65.71	0.916	0.342

A positive real potential is attractive and a positive imaginary potential is absorptive

the (2^+; 4.44 MeV) and δ_3 to the transition to the (3^-; 9.64 MeV) states in ^{12}C.

3 Results and Discussion

The DWBA calculations are performed using the computer code DWUCK4 [12]. The radial integrals have been carried out up to 40 *fm*, in 0.1 *fm* steps with 100 partial waves. We analyzed the angular distribution of differential cross sections for the elastic and inelastic scattering of $K^{\pm}$ from ^{12}C, in terms of three α-clusters with the parameters given in Table 1. The starting parameters which were taken from Ebrahim and Khallaf [10] were used in the search involving all six parameters of the real and imaginary potentials, in groups of two at a time. The best fitting optical model parameters are listed in Table 1. The central optical potential used here is obtained from (9) and inserted into the DWUCK4 program. The obtained results for best fit angular distributions of differential elastic and inelastic cross sections shown in Figs. 1, 2, 4, 5, and 6 are obtained with the parameters of Table 1. The calculated χ^2 values corresponding to each case under consideration are minimum for our potential model at each of these cases.

Examples are taken at momenta ranging from 635 to 800 MeV/c, where the experimental data are available. At the very forward angle, the experiments show that the differential cross sections rise very rapidly, but the calculations converge toward smaller values. This originates from the fact that we have neglected the contribution of Coulomb interaction which is the long-range interaction in the optical potential.

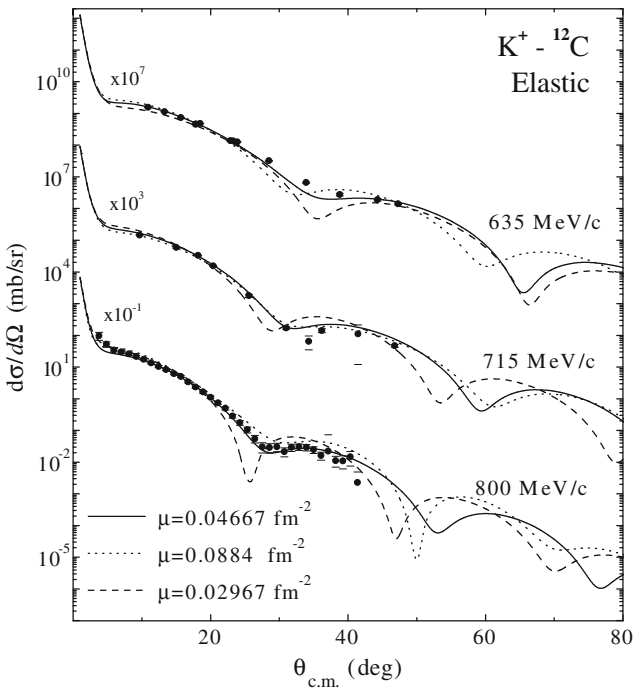

Fig. 1 Differential elastic scattering cross sections for 635, 715, and 800 MeV/c K^+ on ^{12}C. The *solid curve* is the optical potential predictions from the present work with $\mu = 0.04667\ fm^{-2}$, the *dotted curve* is the same calculations but with $\mu = 0.0884\ fm^{-2}$, and the *dashed curve* is the same calculations but with $\mu = 0.02967\ fm^{-2}$. The *solid circles* represent the experimental data taken from Refs. [2, 14]

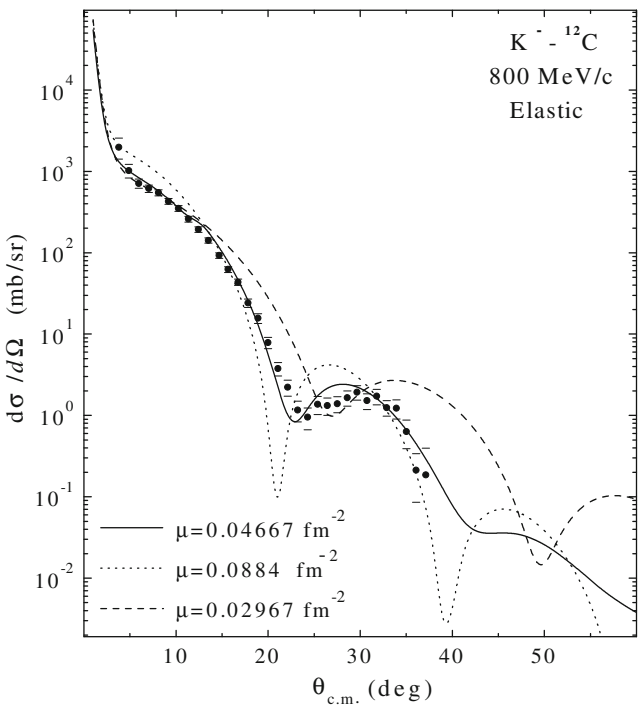

Fig. 2 As in Fig. 1, but for K^- elastic scattering from ^{12}C at 800 MeV/c. The *solid circles* represent the experimental data taken from Ref. [2]

In the study of Khallaf et al. [22], three values of the range parameter of ^{12}C were used namely $\mu = 0.02967$, 0.04667, or 0.0884 fm^{-2}, one of them, $\mu = 0.04667$ fm^{-2}, was calculated through the root mean square radius of ^{12}C taking into account the root mean square radius of alpha particle. Moreover, it produced better fits to ^{12}C ions elastic scattering data from several targets at several energies. To confirm this result, Figs. 1 and 2 show the present fitting of $K^{\pm}$–^{12}C elastic scattering at 635–800 MeV/c kaon lab momenta using the above mentioned different values of μ. Figures 1 and 2 show that $\mu = 0.04667$ fm^{-2} is preferred since it yields a better fitting especially at forward angles. Therefore, we have chosen $\mu = 0.04667$ fm^{-2} for the use in the present calculations. This agrees well with the reported results for the α-particle model of ^{12}C–^{12}C reaction [23]. The resulting real and imaginary optical potentials for K^+ scattered from ^{12}C at 715 MeV/c are shown in Fig. 3. These potentials for ^{12}C are calculated with $\mu =$ 0.0467, 0.02967, and 0.0884 fm^{-2}. From that figure, it is seen that in this case, the real/imaginary part is quite shallow and everywhere attractive/absorptive. These relative shallow potentials for positive kaons compared to pions confirm that K^+ mesons weakly interact with nuclei. The present optical potential of ^{12}C predicts well the maximum and minimum positions with those calculated in the study of Li [24] for the elastic and inelastic scattering differential cross sections at large angles according to the choice of the wave function with $\mu = 0.04667$ fm^{-2}. In particular, our calculations predict two diffraction minima, but the predicted minima are much deeper than those observed.

In Fig. 1, the measured elastic scattering differential cross sections at forward angles and the positions of minima and maxima agree well with our calculations at the three momenta 635, 715, and 800 MeV/c. The differential elastic cross sections of K^- scattered from ^{12}C at 800 MeV/c is shown in Fig. 2. The K^- minima are sharper than those for K^+, but the K^+ data fall more steeply than the K^-. The K^+ minima occur at larger angles (typically by about 5°) than for K^-, indicating that K^+ sees a smaller nucleus than K^-. This agrees well with the reported results in Ref. [2].

Inelastic scattering is another important aspect of the interactions of kaons with nuclei. The α-particle model optical potential may be tested to predict observables of $K^{\pm}$ inelastically scattered from nuclei. In a phenomenological approach, it is expected that both elastic and inelastic scattering will be described in the same framework. This consistency condition may provide more information on the kaon-nucleus potential, and is essential before reliable nuclear structure information

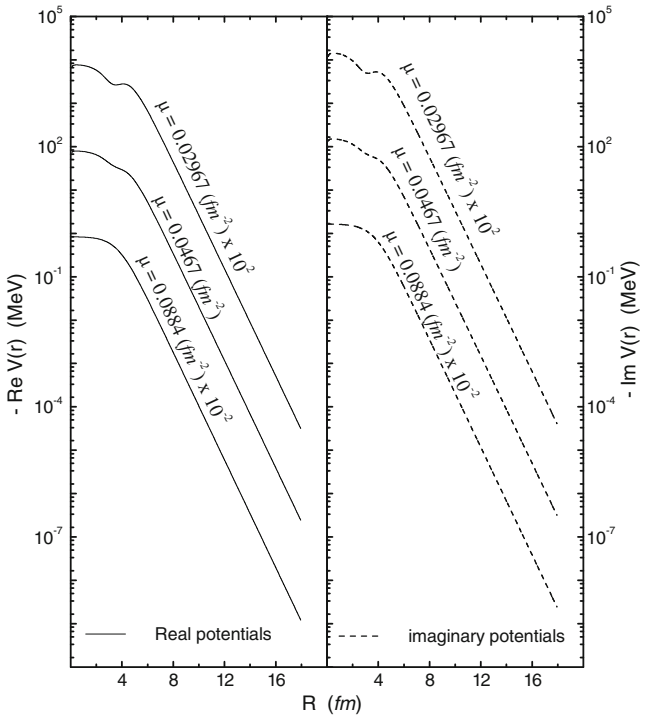

Fig. 3 *Left*, the real parts of the optical potentials for K^+ scattered from ^{12}C at 715 MeV/c. The *full curves* represent the predictions of the expression (9), with $\mu = 0.02967$, 0.04667, and 0.0884 fm^{-2}. *Right*, the same as *left* but for the imaginary parts

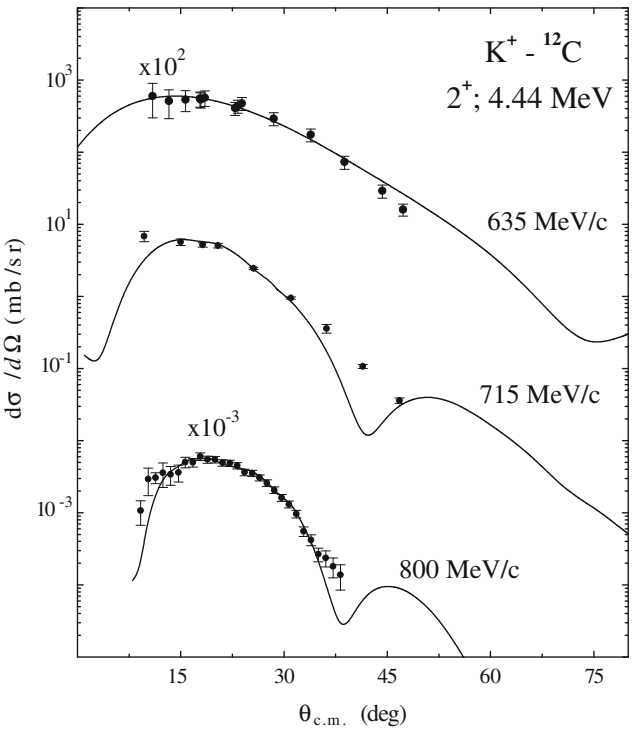

Fig. 4 Differential inelastic scattering cross sections of 635, 715, and 800 MeV/c K^+ leading to the lowest 2^+ state in ^{12}C with the present optical potential with $\mu = 0.04667$ fm^{-2}. The experimental data are taken from Refs. [2, 14]

can be reported. With the zero-range distorted wave Born approximation, we may also compute inelastic scattering to the collective 2^+ and 3^- states of ^{12}C using the standard light ion code DWUCK4 [12].

When the potential is deformed [Eq. (10)] and the value of the deformation length δ_l is adjusted, a reasonable agreement with data can be found as shown in Figs. 4, 5, and 6. Coulomb excitation was found to be unimportant for the inelastic scattering considered here. The resulting deformation lengths determined by visually adjusting the calculations to reproduce the equivalent data listed in Table 2 were compared to those obtained from calculations using parameters given in Refs. [10, 11].

To calculate deformation lengths from parameters of Refs. [10, 11], we used the relations:

$$\delta_r = \beta_l\, r_u\, A^{\frac{1}{3}},$$
$$\delta_i = \beta_l\, r_w\, A^{\frac{1}{3}}, \qquad (11)$$

where β_l, $R_u(= r_u\, A^{1/3})$, and $R_w(= r_w\, A^{1/3})$ are defined and given in Ref. [10]. The deformation lengths extracted from the present calculation are consistent with those obtained by the analysis of the inelastic scattering of K^+ and other particles from ^{12}C as shown in Table 2. In our case, the corresponding values fall between 0.802 and 1.429 *fm* for different momenta.

The extraction of $\delta_{2,3}$ for $K^{\pm}$ inelastic scattering presents an opportunity for investigating possible differences in the proton and neutron distributions in ^{12}C nucleus. No extra neutrons in the ^{12}C nucleus (N = Z) may lead to different values of $\delta^+{}_{2,3}$ and $\delta^-{}_{2,3}$. The shell closure at A = 12 for the 2^+ and 3^- states is collective. The excitation of both proton and neutron particle-hole configurations are equally likely to occur, and no significant difference between δ^+ and δ^- are expected for scattering to either the 2^+ or 3^- state in ^{12}C.

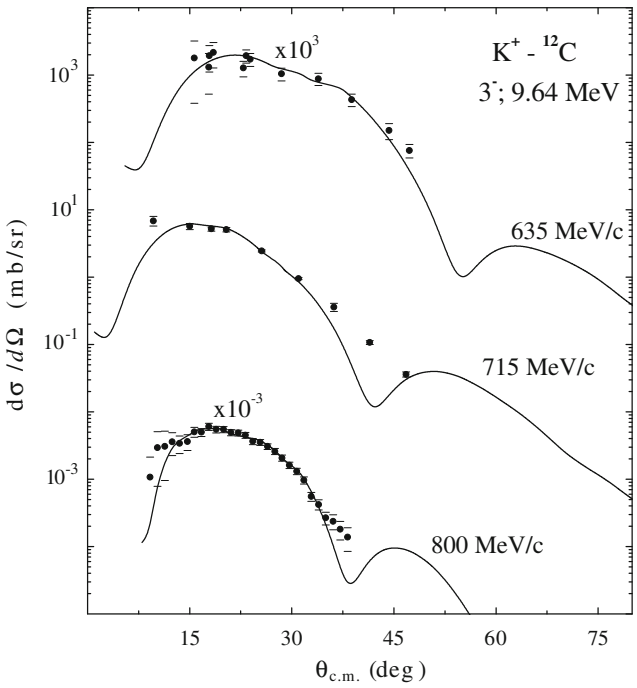

Fig. 5 As in Fig. 3, but for K^+ exciting the 9.64 MeV 3^- state of ^{12}C

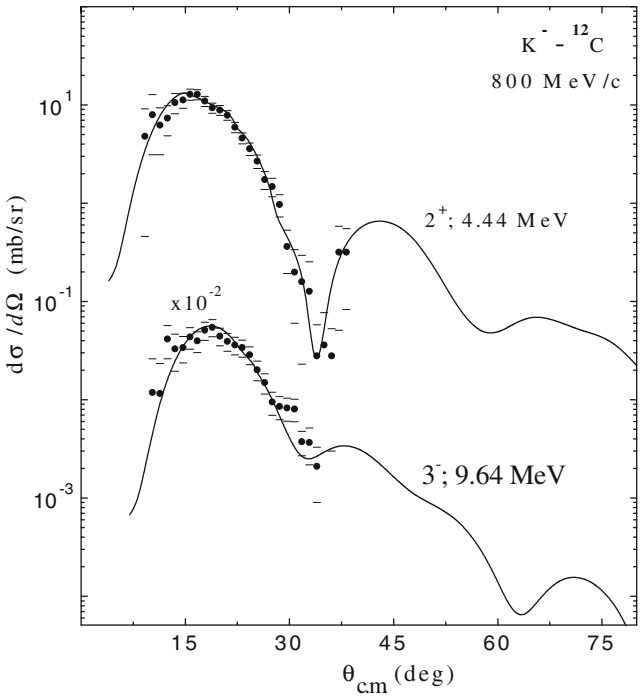

Fig. 6 As in Fig. 2, but for K^- exciting the 4.44 MeV 2^+ and 9.64 MeV 3^- excited states of ^{12}C

The angular distributions for the inelastic scattering of K^+ by ^{12}C (2^+; 4.44 MeV) at 635–800 MeV/c kaon Lab momenta are presented in Fig. 4. The experimental angular distributions and the present calculations are generally smooth, without the presence of well-defined minima. Rather poorer agreement is obtained for calculations of K^+ scattering, due to the strong coupling of the ground state to the 2^+ excited state in ^{12}C at 715 MeV/c in large-angle region. Satisfactory agreement with the measured angular distributions is obtained at 800 MeV/c, although the general shapes of the angular distributions are well reproduced by the present calculations. The peak of the cross sections versus scattering angles shifts forward with increasing momenta.

Also shown in Fig. 5 are angular distributions of the inelastic scattering of K^+ by ^{12}C (3^-; 9.64 MeV) at the three momenta considered here, except for K^+ scattering to the 3^- at 715 MeV/c. Inelastic scattering

Table 2 Deformation lengths δ (in *fm*) from K^+ meson inelastic scattering from ^{12}C compared to those predicted by others

P_{lab}	State	Present		Others				
		δ_r	δ_i	δ_r	δ_i	Ref.	δ	Ref.
635	2^+	1.429	1.029	1.725	1.114	[8]	1.22–1.27 (±0.13)	[25]
				1.522	0.991	[10]	1.03–1.63	[26]
715		1.214	0.921	1.355	1.005	[8]	1.02–1.41	[27]
				1.735	1.014	[10]	1.5–2.1	[28]
800		1.308	0.902	1.413	0.978	[8]	1.0±0.1	[29]
				1.619	1.017	[10]	1.07±0.05	[30]
635	3^-	1.232	0.878	1.449	1.102	[8]	0.65–1.23	[31]
				1.381	0.897	[10]		
715		1.118	0.842	1.302	1.205	[8]		
				1.432	0.866	[10]		
800		1.208	0.802	1.319	0.955	[8]		
				1.358	0.835	[10]		

calculations with the present potential describe the shapes of the inelastic angular distributions better than the calculations of WS with optical parameters fit to the measured elastic scattering data [14].

The theoretical predictions for K^- to the 2^+ and 3^- excited states of ^{12}C 800 MeV/c are found to be in better agreement with data, as shown in Fig. 6. The present calculations based on the WS potential of α clusters of ^{12}C give a better fit to data than the calculations of Marlow et al. [2].

From Table 2, it can be seen that values of deformation lengths determined here using the present potential are very similar to those obtained in Refs. [10, 11]. It is clear from Table 2 that the deformation lengths of the real potential are larger than the corresponding ones for the imaginary potential in all cases under consideration. Moreover, δ_r for the 2^+ and 3^- states at 715 MeV/c given in Table 2 falls adequately close to the corresponding δ from different reactions given in Refs. [25–31]. It can be seen from Table 2 that the values of the imaginary deformation lengths determined here for 2^+ and 3^- excited states in ^{12}C decrease with increasing kaon momenta, except for the case of 715 MeV/c K^+ inelastic scattering off the 3^- state in ^{12}C.

The present potential is also used to predict reaction and total cross sections of $K^\pm$ scattering on ^{12}C from 400 to 1,000 MeV/c. The DWUCK4 program calculates these cross sections. The results of the present model (solid curves) are smaller than calculations based on the Watanabe superposition model (dashed curves) [11] by 3 % for the total and 3–5 % for the reaction cross sections. The two computations are very similar to each other and this is due to that both use the Woods–Saxon shape for both the real and imaginary parts of the kaon–alpha potential (see (5) in Ref. [11]). It can be seen from Fig. 7 that there is a somewhat satisfactory agreement between the present calculations of σ_R for K^+ and data reported in Ref. [32]. This indicates that the imaginary part of the present optical potential used here, which is strongly correlated to σ_R, is well predicted. Since the kaon mean free path λ is proportional to the inverse of the total K-nucleon cross sections, i.e., $\lambda \propto \frac{1}{\sigma_T/A}$ [33], it is easy to see from Fig. 7 that low values of σ_T when compared to the corresponding values for pion scattering [8, 34] indicate longer mean free path for K^+.

In Table 3, reaction and total cross sections and ratios of experimental [32] to calculated cross sections

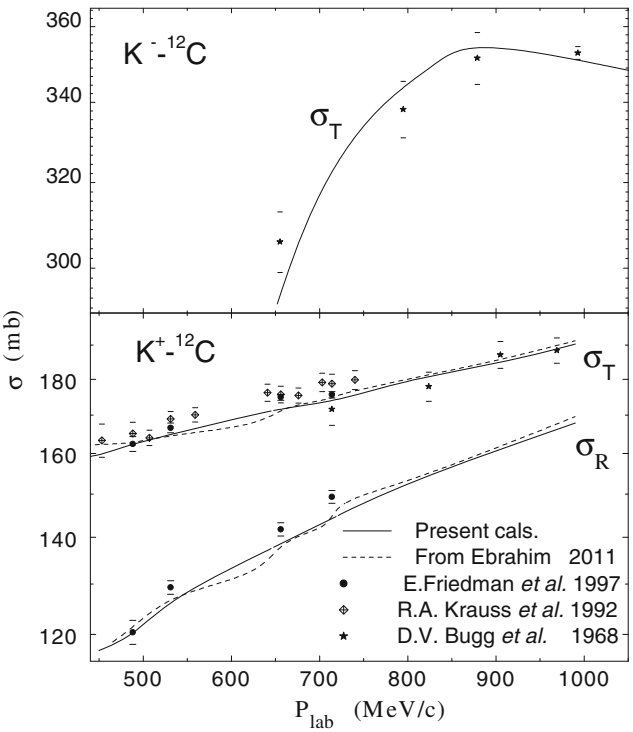

Fig. 7 The *top portion* is for total cross sections for K^--^{12}C. The *lower portion* is for the reaction and total cross sections for K^+-^{12}C. *Solid lines* are from the present work and *dashed lines* are the Watanabe model calculations of Ebrahim [11]. These lines are compared with the data from Friedman et al. [32], Krauss et al. [35], and Bugg et al. [36] for the total and reaction cross sections

Table 3 Reaction and total cross sections and ratios of the experimental to calculated values for K^+ scattering from ^{12}C

P_{lab}	σ_R	σ_T	σ_R(exp.)/σ_R(cal.)	σ_T(exp.)/σ_T(cal.)
450	116.2	156.4		
488	118.2	159.6	1.019	1.017
500	122.2	160.1		
531	126.3	162.8	1.024	1.023
600	133.3	166.5		
656	138.6	169.5	1.023	1.031
700	143.1	170.8		
714	144.6	171.5	1.033	1.024
800	153.2	176.8		

The experimental values are taken from Friedman et al. [32]

are shown for ^{12}C. The results show that both calculated reaction and total cross sections are smaller than experimental data. Calculated reaction cross sections display larger discrepancy with the data than the total cross sections. The ratios in Table 3 display a momentum dependence which can be removed when the values for ^{12}C are referred to those for ^6Li. These super-ratios [32] are then nearly momentum independent. The present calculations are in good agreement with data at low momenta, but they grow less rapidly than the data for higher momenta.

In general, the shapes and magnitudes for the $K^+-^{12}C$ elastic and inelastic cross sections are similar using the present model which is based on the 3α-cluster of ^{12}C and those of Watanabe superposition model which is also based on the α clusters [11], although the two computations do not lead to identical total and reaction cross sections for the $K^+-^{12}C$ scattering at the momentum range considered here.

4 Conclusion

We used a very simplified nonrelativistic optical potential in the present model (with real and imaginary Woods–Saxon folding potentials) to obtain a good description for $K^{\pm}$-^{12}C elastic scattering at 635, 715, and 800 MeV/c kaon lab momenta using the DWBA with DWUCK4 code. The success of the present potential to fit the differential elastic and inelastic cross section data may be due to the fact that the kaon-alpha potential is based on the Woods–Saxon form which was forced to agree with the data.

The differential inelastic scattering of $K^{\pm}$ to the lowest 2^+ and 3^- states in ^{12}C are calculated by the present local potential, and this potential has the ability to reproduce the shape and magnitude of the $K^{\pm}$ scattering data. The deformation lengths determined from the present analysis are in agreement with deformations determined previously using other probes. This collective model analysis is successful in its description of the reaction dynamics and the structure of N=Z nucleus.

In conclusion, the optical model used in the present work can serve as a reliable model for kaon-nucleus scattering.

Acknowledgement I would like to thank Professor A.L. Elattar, Department of Physics, Assiut University, for a careful reading of the manuscript.

References

1. C.B. Dover, P.J. Moffa, Phys. Rev. C **16**, 1087 (1977)
2. D. Marlow, et al., Phys. Rev. C **25**, 2619 (1982)
3. C.M. Chen, D.J. Ernst, Phys. Rev. C **45**, 2019 (1992)
4. M.F. Jiang, D.J. Ernst, C.M. Chen, Phys. Rev. C **51**, 857 (1995)
5. P.B. Siegel, W.B. Kaufmann, W.R. Gibbs, Phys. Rev. C **31**, 2184 (1985)
6. G.E. Brow, C.B. Dover, P.B. Siegel, W. Weise, Phys. Rev. Lett. **60**, 2723 (1988)
7. R.J. Peterson, A.A. Ebrahim, H.C. Bhang, Nucl. Phys. A **625**, 261 (1997)
8. A.A. Ebrahim, S.A.E. Khallaf, Phys. Rev. C **66**, 044614 (2002)
9. L.S. Kisslinger, Phys. Rev. **98**, 761 (1955)
10. A.A. Ebrahim, S.A.E. Khallaf, J. Phys. G **30**, 83 (2004)
11. A.A. Ebrahim, Eur. Phys. J. A **47**, 74 (2011)
12. P.D. Kunz, computer code DWUCK4, University of Colorado (1996), http://spot.colorado.edu/~kunz/. Accessed 11 Sept 2011
13. G.R. Satchler, Nucl. Phys. A **540**, 533 (1992)
14. R.E. Chrien, et al., Nucl. Phys. A **625**, 251 (1997)
15. A.A. Ebrahim, Braz. J. Phys. **41**, 146 (2011)
16. K.G. Boyer, et al., Phys. Rev. C **24**, 598 (1981)
17. K.G. Boyer, et al., Phys. Rev. C **29**, 182 (1984)
18. C.L. Morris, et al., Phys. Rev. C **24**, 231 (1981)
19. G.R. Satchler, W.G. Love, Phys. Rep. **55**, 183 (1979)
20. M.W. Kermode, Proc. Phys. Soc. **84**, 557 (1964)
21. S.A.E. Khallaf, M. El-Azab, Atomkernenergie/Kerntechnik **37**, 294 (1981)
22. S.A.E. Khallaf, A.L. El-Attar, M. El-Azab Farid, J. Phys. G **8**, 1721 (1982)
23. S.A.E. Khallaf, M. Abdelrahman, S. Abdelraheem, S. Mahmoud, Jpn. J. Appl. Phys. **37**, 657 (1998)
24. Li Qing-Run, Nucl. Phys. A **415**, 445 (1984)
25. S.A.E. Khallaf, A.M.A. Nossair, A.A. Ebrahim, A.A. Ebraheem, Nucl. Phys. A **714**, 412 (2003)
26. A. Nadasen, M. McMaster, M. Fingal, J. Tavormina, J.S. Winfield, R.M. Ronningen, P. Schwandt, F.D. Becchetti, J.W. Jánecke, R.E. Warner, Phys. Rev. C **40**, 1237 (1989)
27. A.S. Dem'yanova, E.F. Svinareva, S.A. Goncharov, S.N. Ershov, F.A. Gareev, G.S. Kazacha, A.A. Ogloblin, J.S. Vaagen, Nucl. Phys. A **542**, 208 (1992)

28. P.J. Moffa, C.B. Dover, J.P. Vary, Phys. Rev. C **16**, 1857 (1977)
29. D.I. Pham, R. de Swiniarski, Z. Phys. A **326**, 309 (1987)
30. M.E. Brandan, K.W. McVoy, Phys. Rev. C **43**, 1140 (1991)
31. S.M. Smith, G. Tibell, A.A. Cowley, D.A. Goldberg, H.G. Pugh, W. Reichart, N.S. Wall, Nucl. Phys. A **207**, 273 (1973)
32. E. Friedman, et al., Phys. Rev. C **55**, 1304 (1997)
33. C.B. Dover, G.E. Walker, Phys. Rep. **89**, 1 (1982)
34. A. Saunders, S. Høibråten, J.J. Kraushaar, B.J. Kriss, R.J. Peterson, R.A. Ristinen, J.T. Brack, G. Hofman, E.F. Gibson, C.L. Morris, Phys. Rev. C **53**, 1745 (1996)
35. R.A. Krauss, et al., Phys. Rev. C **46**, 655 (1992)
36. D.V. Bugg, et al., Phys. Rev. **168**, 1466 (1968)